BEST AVAILABLE IMAGES

Defective images within this document are accurate representations of the original documents submitted by the applicant.

Defects in the images may include (but are not limited to):

- BLACK BORDERS
- TEXT CUT OFF AT TOP, BOTTOM OR SIDES
- FADED TEXT
- ILLEGIBLE TEXT
- SKEWED/SLANTED IMAGES
- COLORED PHOTOS
- BLACK OR VERY BLACK AND WHITE DARK PHOTOS
- GRAY SCALE DOCUMENTS

IMAGES ARE BEST AVAILABLE COPY.

As rescanning documents *will not* correct images, please do not report the images to the Image Problem Mailbox.

Journal of Molecular Neuroscience

ISSN0895-8696/00/14:93–105/$13.25

Synaptogenesis and Myopathy Under Acetylcholinesterase Overexpression

Efrat Lev-Lehman,[1,**] Tamah Evron,[1] Ron Shraga Broide,[1,**] Eran Meshorer,[1] Ilana Ariel,[1,2] Shlomo Seidman,[1] and Hermona Soreq*[,1]

[1]Department of Biological Chemistry, The Life Sciences Institute, The Hebrew University of Jerusalem, Jerusalem, Israel 91904; [2]Department of Pathology, Hadassah University Hospital, Mount Scopus, Jerusalem, Israel

Abstract

Environmental, congenital, and acquired immunological insults perturbing neuromuscular junction (NMJ) activity may induce a variety of debilitating neuromuscular pathologies. However, the molecular elements linking NMJ dysfunction to long-term myopathies are unknown. Here, we report dramatically elevated levels of mRNA encoding *c-Fos* and the "readthrough" (R) variant of acetylcholinesterase (AChE) in muscles of transgenic mice overexpressing synaptic (S) AChE in motoneurons and in control mice treated with the irreversible cholinesterase inhibitor diisopropylfluorophosphonate (DFP). Tongue muscles from DFP-treated and AChE-S transgenic mice displayed exaggerated neurite branching and disorganized, wasting fibers. Moreover, diaphragm muscles from both transgenic and DFP-treated mice exhibited NMJ proliferation. 2′-O-methyl-protected antisense oligonucleotides targeted to AChE mRNA suppressed feedback upregulation of AChE and ameliorated DFP-induced NMJ proliferation. Our findings demonstrate common transcriptional responses to cholinergic NMJ stress of diverse origin, and implicate deregulated AChE expression in excessive neurite outgrowth, uncontrolled synaptogenesis, and myopathology.

Index Entries: Acetylcholinesterase/antisense; cholinesterase inhibitors; physiological stress; muscle pathology; neuromuscular junction.

*Author to whom all correspondence and reprint requests should be addressed.

**Current address: Departments of Human and Molecular Genetics (E.L.L.) and Neuroscience (R.S.B), Baylor College of Medicine, Houston, TX

Introduction

Neuromuscular junctions (NMJ) are highly specialized, morphologically distinct, and well-characterized cholinergic synapses (Sanes and Lichtman, 1999). Chronic impairments in NMJ activity induce neuromuscular disorders characterized by deterioration of muscle structure and function. Thus, etiologically diverse insults interfering with acetylcholine-mediated neurotransmission cause a variety of "myasthenic" syndromes presenting muscle weakness and fatigue (Livneh et al., 1988; Schonbeck et al., 1990; Engelhart et al., 1997; Donger et al., 1998; Lindstrom, 1998). The molecular and cellular mechanisms leading from compromised NMJ activity to muscle wasting have not been elucidated. However, it is likely that physiological stress imposed on the nerve and/or muscle under conditions of NMJ dysfunction initiate changes in gene expression. Inhibitors of the acetylcholine-hydrolyzing enzyme, AChE, induce neuromuscular pathologies sharing features with the myasthenic syndromes. Among the delayed effects of anticholinesterase intoxication are degeneration of synaptic folds, terminal nerve branching, enlargement of motor endplates, and disorganization of muscle fibers (Laskowski et al., 1975; Kawabuchi et al., 1976). Cholinesterase inhibitors promoting myopathy include organophosphate poisons such as DFP and paraoxon (the toxic metabolite of the agricultural insecticide parathion), and carbamate drugs like pyridostigmine and neostigmine, used to treat myasthenia gravis (Evoli et al., 1996). The similarities between the neuromuscular impairments resulting from anticholinesterase exposure and that of pathophysiological NMJ dysfunction suggest overlapping and/or convergent pathways involving AChE.

RNA transcribed from the mammalian *ACHE* gene is subject to 3′ alternative splicing yielding mRNAs encoding a "synaptic" (S) isoform, a "erythropoietic" (E) isoform, and the stress-related "readthrough" AChE-R derived from the 3′-unspliced transcript (Ben Aziz-Aloya et al., 1993; Massoulie et al., 1993). In addition to their hydrolytic activities, the various AChEs exert sequence-specific morphogenic effects on neurite outgrowth (Layer et al., 1995; Koenigsberger et al., 1997; Grifman et al., 1998; Sharma et al., 1998; Sternfeld et al., 1998) and NMJ structure (Shapira et al., 1994; Seidman et al., 1995). Transgenic mice overexpressing human AChE-S in spinal cord motoneurons displayed progressive neuromotor impairments that were associated with changes in NMJ ultrastructure (Andres et al., 1997, 1998). However, the molecular mechanisms mediating neuromuscular deterioration in these mice were unclear. Elevated intracellular calcium was previously implicated in anticholinesterase-mediated myopathologies (Laskwoski et al., 1975). Electromyography (EMG) data revealed exaggerated post-synaptic responses in muscles of transgenic mice that indicated similarly enhanced calcium influx. In rodent brain, we found that both stress and cholinesterase inhibitors induce dramatic calcium-dependent overexpression of AChE-R (Kaufer et al., 1998). We therefore predicted that feedback overexpression of AChE-R would also occur in muscles of both anticholinesterase-treated control and NMJ-stressed AChE transgenic mice. Moreover, we expected that overexpressed AChE would have morphogenic implications for the nerves and/or muscles. To test these hypotheses, we examined AChE expression, motor endplate organization, neurite outgrowth, and muscle integrity in AChE-S transgenic mice and in normal mice treated with DFP with or without coadministration of antisense oligonucleotides to AChE mRNA. Our findings identify the AChE feedback loop as a molecular response common to both physiological NMJ stress and anticholinestrase exposure in muscle. Furthermore, they suggest that induced overexpression of AChE-R contributes to neuromuscular deterioration under diverse conditions leading to disease and demonstrate in vivo antisense blockade of the AChE feedback response to NMJ stress.

Materials and Methods

Animals and Tissue Preparations

FVB/N mice, aged postnatal day (P) 0, 15, 30 and 4 mo (M) were sacrificed and their tongues removed into liquid nitrogen for polymerase chain reaction (PCR) and biochemical analyses. For *in situ* hybridization and silver staining, 2-mm^3 cubes of tongue tissue were incubated in 3.7% formaldehyde overnight at room temperature and then

paraffin embedded. Sections were cut (5 ³ m) and placed on 3-aminopropyltriethoxysilane-treated slides, dried at 37°C overnight, and kept at 4°C until use. For cytochemistry, whole diaphragms were fixed for 1 h in 4% paraformaldehyde at 22°C, rinsed twice in phosphate-buffered saline (PBS), and stained for catalytically active AChE activity as previously described (Andres et al., 1997).

Chronic DFP Treatment

Mouse pups were housed with the dam in a light- and temperature-controlled room. Animals were injected subcutaneously (s.c.) once daily with either 1.0 mg/kg DFP (Aldrich Chemical Co., Milwaukee, WI) dissolved in corn oil or with corn oil alone during the first 2 postnatal weeks. To minimize central nervous system (CNS) toxicity, pups were pretreated with 10 mg/kg (ip) atropine sulfate (Sigma Chemical Co., St. Louis, MO) in saline 15 min before injection. At P15, about 4 h after the last injection, pups were sacrificed and their tongues removed.

DFP/Antisense Experiments

Adult FVB/N mice were coinjected intraperitoneally (ip) once daily for 4 consecutive days with DFP alone or together with 5 ³ g/kg of an antisense oligonucleotide (AS3; 3˜CCA GCT TCT TTT ATA ACG TCs) targeted to exon E2 in the mouse acetylcholinesterase gene. AS3 included 2˜-O-methyl ribonucleotide substitutions at the three 3˜-terminal positions to stabilize it against nucleolytic degradation.

RT-PCR Analysis

RNA from tongue samples was extracted by RNA Clean (PeqLAb, Heidelberg, Germany) according to manufacturer's instructions. Reverse transcription (RT)-PCR reactions were performed as previously described using a common upstream (+) primer and downstream (–) primers selective for each of the alternative AChE mRNA exons (Fig. 1A):

E3: 1361(+) {5˜-CCGGGTCTATGCCTACAT-CTTTGAA-3˜}
E6: 1844(–){5˜CACAGGTCTGAGCAGCGCTCC-TGCTTG-CTA-3˜}
E5: 240(–) {5˜-AAGGAAGAAGAGGAGGGA-CAGGGCTAAG-3˜}
I4: 74(–) {5˜-TTGCCGCCTTGTGCATTCCCT-3˜}

To detect *c-Fos* mRNA, we used the primer pair 1604(+)/2306(–) (Kaufer et al., 1998). PCR products sampled every third cycle from cycles 24–36 for the AChE and *c-Fos* mRNAs, and from cycles 18–24 for ¾actin mRNA were electrophoresed on 1.5% agarose gels and stained with ethidium bromide.

In Situ *Hybridization*

2˜-O-methylated, 5˜-biotinylated cRNA probes were used to decorate selectively alternative mouse (m) AChE mRNAs. Detection was with alkaline phosphatase-conjugated streptavidin and ELF™ detection kit (Molecular Probes).

mI4: (–79) 5˜-AACCCUUGCCGCCUUGUG-CAUUCCCUGCUCCCCCCACUCCAUGCGC-CUA-C-3˜(–29);
mE6: (209)5˜-CCCCUAGUGGGAGGAAGUCG-GGGAGGAGUGGACAGGGCCUGGGGGCU-CGG-3˜(258);
mE5: (–249) 5˜-GAGGAGGAAAAGGAAGAA-GAGGAGGGACAGGGCUAAGUCCGGCCC-GGGC-3˜(–200);

Paraffin-embedded tongue sections were deparaffinized and dehydrated in a methanol/PBT (PBS, 0.1% Tween-20) series. Hybridization included preclearing in H_2O_2 (6% in PBT, 30 min), proteinase treatment, glycine wash, and refixation (4% paraformaldehyde, 20 min), all essentially as described elsewhere (Kaufer et al., 1998; Grisaru et al., 1999) except that 1% sodium dodecyl sulfate (SDS) was added to the hybridization buffer and to solution 1 and 0.1% Tween-20 was added to solution 2.

Neurites Silver Stain

Paraffin-embedded tongue muscle sections were stained for neuronal fibers using silver nitrate (20%, 60 min at 37°C), distilled water washes and incubation in ammonium hydroxide-silver nitrate solution (60 min). Color was developed for 24–36 h. For fixation, slides were dipped in sodium thiosulfate (2 s), washed in water, and dehydrated.

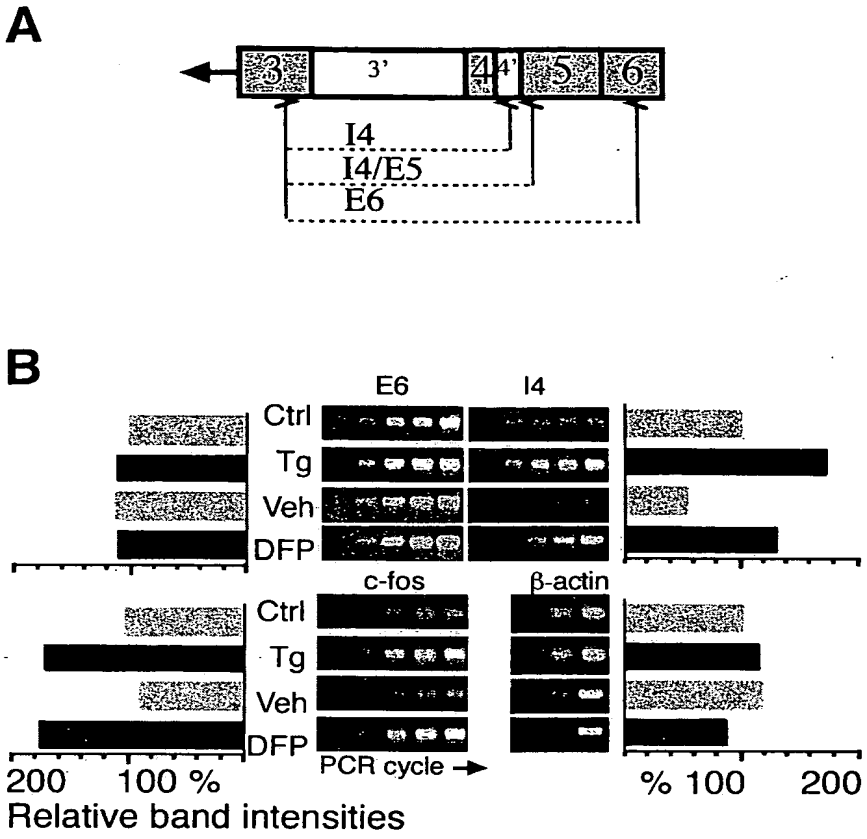

Fig. 1. Transgenic AChE-S and DFP similarly induce enhanced c-fos and AChE-R mRNA production in muscle. **(A)** The mouse ACHE gene and alternative splicing products. Presented is a schematic illustration of coding exons 3, 4, 5, and 6 (shaded boxes) and introns 3 to 4 (white boxes) in the mouse ACHE gene. The "synaptic" AChE-S mRNA transcript (E6) results from splicing of exons 4 to 6; the "erythropoietic" AChE-H mRNA transcript (E5) from splicing of exons 4 to 5; *readthrough* AChE-R mRNA retains intron I4 in a mature unspliced transcript. Arrowheads indicate PCR primer pairs detecting the individual mRNA transcripts. **(B)** RT-PCR analyses. RT-PCR was performed using primers specific for the various alternative AChE mRNAs (*See* Materials and Methods section). Presented are PCR products of AChE mRNA derived from tongue muscle of control (Crtl) or AChE transgenic (Tg) newborn mice or from control mice treated for 2 wk with either DFP or vehicle (Veh). Note the increased levels of both endogenous mouse ACLE-R and c-fos mRNAs in transgenic vs control mice and in control mice injected with DFP. Neither endogenous AChE-S or the unrelated ¾-actin mRNAs responded to either transgenic AChE overexpression or AChE inhibition. Displayed are PCR reactions sampled every third cycle from cycle 24 for AChE and c-fos, and from cycle 18 for ¾-actin. One of four experiments for each mRNA using different RNA preparations is presented. Bar graph represents the relative band intensity for each mRNA in the presented PCR images as determined by densitometric analysis. Quantification was performed at cycle 33 for AChE and c-fos mRNAs and at cycle 24 for ¾-actin mRNA, within the exponential phase of product accumulation.

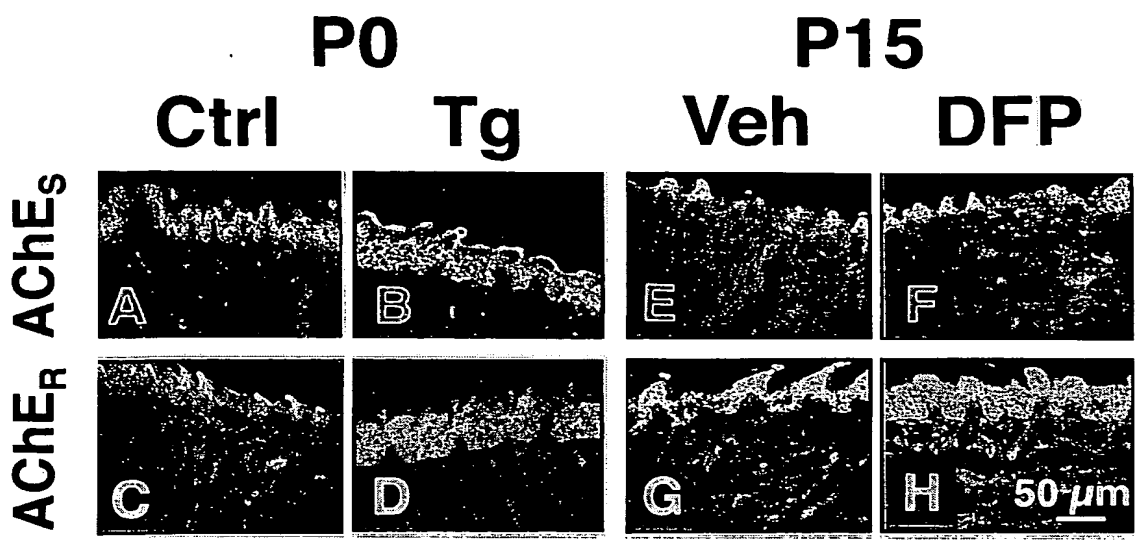

Fig. 2. Overexpressed transgenic AChE-S and DFP induce accumulation of endogenous AChE-R mRNA in both epithelium and muscle. *In situ* hybridization was performed on 7-^{3} m sections of tongue from newborn (P0) control (**A,C**) and AChE-transgenic (**B,D**) mice, or 15-d-old (P15) control mice injected with either vehicle (**E,G**) or the AChE inhibitor DFP (**F,H**). Note enhanced and delocalized fluorescent labeling of AChE-R but not AChE-S mRNA in epithelial cells and muscle fibers from both transgenic and DFP-treated mice as compared to controls.

Results

Chronic Cholinesterase Blockade and Transgenic Overexpression of Synaptic Neuronal AChE Promote Elevated c-Fos *and* readthrough *AChE mRNAs in Muscle*

Both acute stress and cholinesterase inhibitors were shown to trigger overexpression of AChE-R in rodent brain via a c-fos-mediated pathway (Kaufer et al., 1998). To investigate whether the AChE feedback loop is active in muscle, we performed RT-PCR on mRNA extracted from tongue of 2-wk-old (P15) mice injected daily, from birth, with 1 mg/kg DFP. This dose of DFP blocked approx 80% of muscle AChE activity, but did not elicit overt symptoms of cholinergic poisoning. In parallel, RT-PCR was performed on tongue RNA from transgenic mice overexpressing AChE-S in spinal cord motoneurons. Semi-quantitative analyses performed with primers detecting mouse mRNAs encoding either *c-fos* or AChE-R revealed over twofold elevated levels of both transcripts following either chronic inhibition or congenital overexpression of AChE (Fig. 1). In contrast, neither endogenous AChE-S- nor AChE-E-mRNA levels were detectably affected by either DFP or transgenic AChE (Fig. 1 and data not shown). ¾actin mRNA displayed similar levels among all groups, indicating equal starting amounts of RNA in all reactions (Fig. 1). These data demonstrated that both-chronic overproduction and acute blockade of AChE catalytic activity stimulate selective *de novo* synthesis of AChE-R in muscle.

Readthrough *AChE mRNA Accumulates in Both Muscle and Epithelium Under Cholinesterase Blockade and Transgenic AChE Overexpression*

To determine the localization of induced AChE-R mRNA in tongue, we employed high resolution, fluorescent *in situ* hybridization. Fluorescent hybridization signals obtained using an AChE-S mRNA-specific probe exhibited similar moderate intensities and bandwidth in epithelium of newborn transgenic and control mice (Fig. 2A,B). AChE-E mRNA was also detected at low levels in the epithelium of both control and transgenic mice

(not shown). AChE-R mRNA was barely detectable in sections from control mice, consistent with the PCR data. In contrast, pronounced expression of AChE-R mRNA was observed in tongue epithelium of newborn transgenic mice (figure 2C,D). With DFP, no significant differences were observed in the expression of AChE-S mRNA in treated- vs vehicle-injected mice (Fig. 2E,F). However, 15-d-old DFP-treated, but not their littermate controls, exhibited high levels of AChE-R mRNA across the entire width of the tongue epithelium, extending into the muscle (Fig. 2G,H). In general, hybridization with the AChE-S mRNA probe gave moderate and somewhat punctuated staining, consistent with the localization of this message around junctional nuclei (Jasmin et al., 1993). In contrast, staining with the AChE-R mRNA-specific probe yielded a more diffuse staining pattern, especially following DFP treatment, suggesting extrajunctional synthesis. These data demonstrated that both transgenic overexpression and inhibitor-mediated blockade of AChE promote a specific induction of AChE-R mRNA that takes place in both muscle and epithelium.

Transgenic Mice Display Delocalized Overexpression of Catalytically Active AChE in Muscle

High-salt/detergent extracts of tongue revealed a developmental increase in AChE enzyme activity in control mice (12 ± 2 nmol substrate hydrolyzed/min/mg protein at P7 versus 24 ± 4 at P15; $n = 8$). Two-fold increased levels of catalytically active AChE were observed in tongue homogenates from transgenic over control mice at P7, but only 25% at P15. These findings suggested that adjustments in the feedback response take place over time and/or during development. To localize overexpressed AChE in the tongue, we performed cytohistochemical staining for AChE on sections from 1-mo-old control and transgenic mice. In control mice, activity staining was pale except for intense, highly localized staining observed at motor endplates (Fig. 3A,B). In contrast, transgenic mice displayed overall darker staining of the muscle layers, particularly near the submucosal epithelium (Fig. 3C). In transgenic mice, intense staining was observed along muscle fibers, not restricted to endplate regions (Fig. 3D). This staining pattern

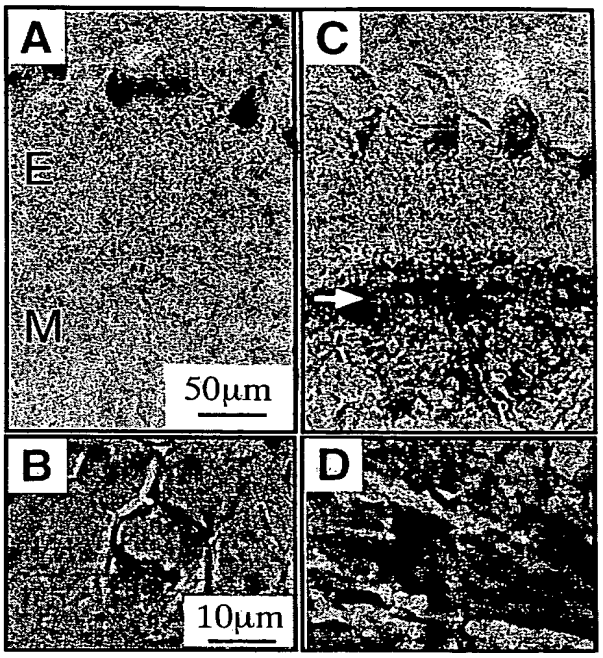

Fig. 3. AChE-Transgenic mice display pronounced nonjunctional enzyme activity in muscle. Tongue sections from 1-mo-old control and transgenic mice were stained for catalytically active AChE. **(A)** At low magnification, diffuse, light staining of both epithelium (E) and muscle (M) layers was observed in sections from control mice **(B)**. Higher magnification revealed strong AChE activity localized to motor endplates **(C)**. In sections from transgenic mice, minimal levels of AChE are visible in the epithelium, (C, arrow; **D**) whereas intense staining is evident in the muscle layer, widely distributed along muscle fibers.

was reminiscent of AChE-S overexpressed in myotomes of microinjected *Xenopus* embryos (Seidman et al., 1995). The relative contributions of endogenous AChE-R and transgenic AChE-S isoforms to this overexpression pattern were not discernable in this experiment. Nevertheless, AChE-R mRNA displayed pronounced overexpression in epithelium of transgenic mice that contrasted with the accumulation of catalytically active protein that was primarily limited to muscle.

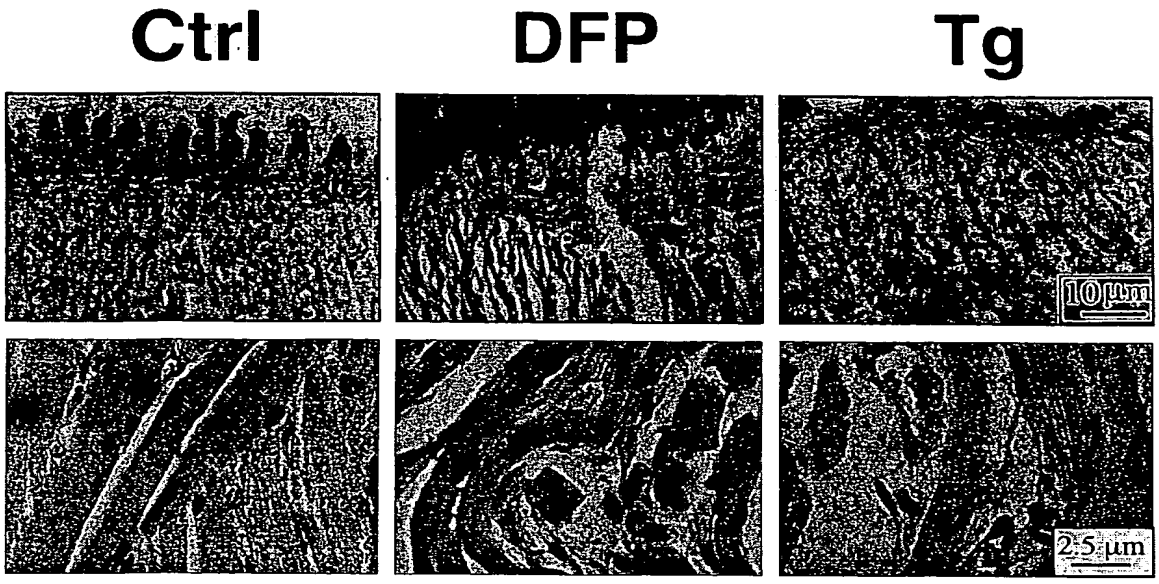

Fig. 4. Transgenic and DFP-induced AChE excesses associated with muscle pathologies. Tongue muscle from P15 untreated control (Ctrl), chronic-DFP-treated control (DFP), or untreated ACHE transgenic (Tg) mice was stained with hematoxyllin-eosin and evaluated for gross morphological features. Muscle tissue of control mice displayed a high degree of organization, with fibers closely aligned in regular parallel arrays. In control mice injected daily with DFP, and in untreated transgenic mice, the corresponding tissues appeared distorted, with apparently atrophic, disorganized muscle fibers. Upper panels present low magnification photomicrographs that include epithelial and muscle layers. Lower panels display high magnification of the muscle layer alone.

Cholinesterase Inhibition and Overexpressed AChE Cause Similar Muscle Pathologies

We previously reported aberrant NMJ ultrastructure and progressive neuromotor dysfunction among adult AChE transgenic mice. We hypothesized that induced AChE-R contributes to this neuromuscular deterioration. In that case, DFP, as an instigator of the AChE feedback loop, would be expected to elicit parallel myopathologies. To determine if the ability of cholinesterase inhibition to promote deterioration of muscle is correlated with overexpressed AChE-R, we studied the gross morphological features of tongue muscle. Muscle fibers from 15-d-old untreated control mice were organized in a linear fashion within parallel bundles. In contrast, muscle fibers from both DFP-treated of the FVB/N strain mice and ACHE-transgenic mice displayed chaotic disorder (Fig. 4). At higher magnification, severely atrophic, vacuolated muscles could be observed in both experimental systems. Despite these muscle malformations, transgenic pups suckled normally and displayed normal growth in their first weeks, suggesting a fairly large safety margin for nonstrenuous muscle activity.

Both Transgenic and Anti-AChE Insults Cause Excessive Muscle Reinnervation

Neurite-growth promoting activities have been demonstrated for AChE in vitro. We therefore hypothesized that overexpressed AChE may exert morphogenic activities on motoneurons. To test this hypothesis, we used silver staining to characterize the distribution of motor axons in tongue muscle from DFP-treated FVB/N and untreated AChE transgenic mice as compared to untreated control mice. Large bundles of neurites (Fig. 5A) were observed in muscles of all three groups in similar numbers, suggesting similar primary nerve input to the tongue in all mice. However, both DFP-

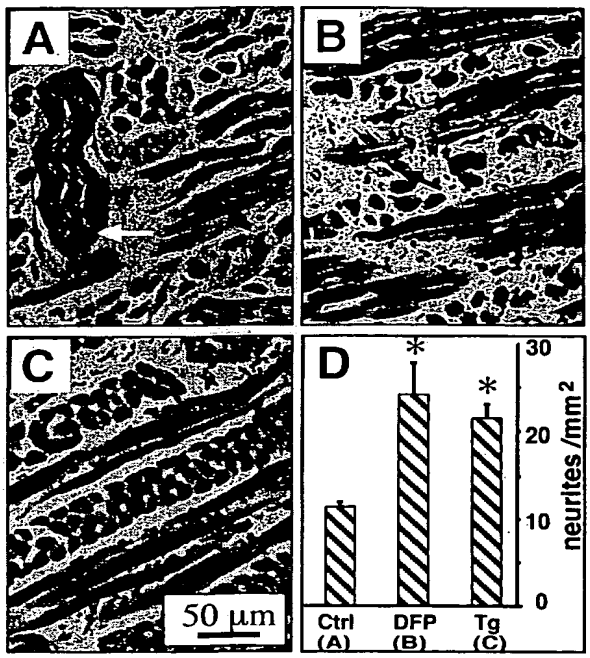

Fig. 5. Both transgenic AChE and DFP induce neurite sprouting. Silver-stained tongue-muscle neurites are shown in parallel sections from **(A)** 15-d-old control, **(B)** DFP-injected control, and **(C)** AChE transgenic mice. Both DFP-treated and transgenic mice displayed numerous small (<200 ^{3} m^2) bundles of neurites as compared with untreated controls (black arrows). Shown are representative photomicrographs in an equivalent location beneath the tongue epithelium. White arrow indicates a representative large (>1000 ^{3} m^2) neurite bundle observed in all groups in similar numbers. Sections from vehicle-injected animals were indistinguishable from untreated controls (not shown). Bar graph represents number of small neurites per mm^2 (average ± SEM) for at least three animals from each group. Asterisk indicates statistically significant difference compared to control ($p < 0.05$, ANOVA)

injected and AChE transgenic mice displayed twofold increases in the number of small (<200 ^{3} m^2), apparently unbundled neurites as compared to both untreated and vehicle-injected controls (Fig. 5B,C). These results indicated axon branching in AChE-R overexpressing muscles, and hinted at a process of denervation-reinnervation in muscles of both DFP-treated and ACHE transgenic mice.

Elevated AChE Induces Antisense-Blocked Expansion of Motor Endplate Fields

The observed increase in small, silver-stained neurites in transgenic and DFP-treated mice suggested that cholinergic insults may be associated with reinnervation processes and the formation of new endplates. To examine this possibility, we counted motor endplates in intact diaphragms from adult control and transgenic mice, and from control mice 1 mo following a course of four daily ip injections of DFP (1 mg/kg). In diaphragms from DFP-treated mice, we observed a twofold increase over controls in the average number of endplates per mm^2 as measured along the length of the innervating nerve (16.14 ± 2.44 vs 8.52 ± 2.42 [±SEM]) (Fig. 6A,B). In diaphragms from transgenic mice, we observed a 50% increase in the density of motor endplates compared to controls (12.61 ± 0.49 NMJs/mm^2) (Fig. 6C). Overall, these endplates appeared smaller than endplates from control mice. However, in addition to the many small endplates, we often observed abnormal, elongated endplates in muscles from both DFP-treated and transgenic mice. Two weeks after treatment with DFP, muscles from FVB/N mice displayed AChE activity that was elevated approximately twofold above controls (10.2 ± 2.3 vs 6.1 ± 2.1 nanomoles substrate hydrolyzed/min/mg tissue; $n \geq 6$). However, coadministration of as little as 80 ^{3} g/kg of a 3$^-$-end-capped, 2$^-$-O-methyl antisense oligonucleotide antisense against AChE (Grisaru et al., 1999) prevented accumulation of catalytically active enzyme by 60% and largely suppressed DFP-induced increases in the number of diaphragm motor endplates; Fig. 6D). AS3 alone reduced NMJ densities to values well below those measured in control muscles without dramatically altering AChE activity. Together with data indicating a relative sensitivity of AChE-R mRNA over AChE-S mRNA to AS3-mediated destruction (Grisaru et al., 1999; Golyam et al., manuscript in preparation), these observations suggest that AChE-R represents a minor but physiologically significant component of total muscle AChE in control untreated animals.

Discussion

We observed common molecular and cellular responses in mouse muscle to transgenic overex-

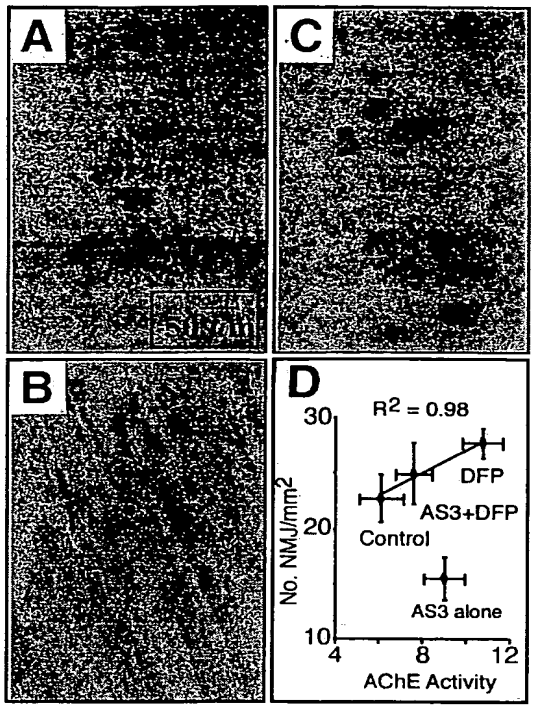

Fig. 6. Transgenic AChE and DFP promote proliferation of motor endplates. Diaphragm motor endplates from **(A)** 4 mo-old control mice, **(B)** control mice 1 mo following repeated treatment with DFP, and **(C)** AChE-transgenic mice visualized by staining for catalytically active AChE. Both DFP-treated control mice and AChE-transgenic mice displayed an increased number of small synapses as compared to controls. **(D)** Graph represents the number of synapses (average ± SEM; $n \geq 3$) per mm^2 tissue as a function of AChE catalytic activity (average ± SEM; $n \geq 6$) as determined in high salt/detergent extracts by the acetylthiocholine colorimetric assay (Seidman et al., 1995). AChE activity is expressed as nanomoles acetylthiocholine hydrolyzed/min/mg tissue. Note that the NMJ/activity ratio in diaphragms from AS3-treated control mice deviates significantly from that expected given the correlation established in the DFP + AS3 paradigm.

pression of neuronal AChE and to chronic administration of the potent AChE inhibitor DFP. On the surface, the convergent outcome of these two experimental manipulations appears paradoxical. DFP imposes a rapid, irreversible blockade of the acetylcholine-hydrolyzing activity of AChE, leading to acetylcholine excess and cholinergic excitation (Taylor, 1995; Friedman et al., 1996). In contrast, transgenic overexpression of AChE in motoneurons is predicted to elevate locally acetylcholine-hydrolyzing activity at the NMJ, presumably resulting in an acetylcholine deficit and cholinergic hypoactivity. Yet, in both cases, we observed elevated levels of *c-fos* and AChE-R mRNAs associated with changes in the number and structure of motor endplates, branching of motor axons, and severe myopathologies. These findings suggest that both gain and loss of synaptic activity impose a physiological stress on the muscle that is translated into changes in gene expression having long-term implications for neuromuscular function. In transgenic mice, abnormally intense electrophysiological activity suggested that long-term adaptation to overexpressed synaptic AChE promotes enhanced cholinergic activity at some sites (Andres et al., 1997; Farchi et al., unpublished data). In that case, even normal neuromotor activity would elicit cholinergic hyperexcitation and induce expression of AChE-R in muscles of transgenic mice. Nevertheless, AChE overexpression following either stress or anticholinesterase intoxication carries dire implications for neuromuscular structure and function in vivo. These findings in muscle parallel the overexpression of AChE-R observed in rodent brain under stress and anticholinesterase exposure. The profound impact of AChE-R overexpression on the structure and organization of NMJs, advances the notion that overexpressed AChE-R in the CNS plays a role in the delayed psychopathologies associated with trauma or anticholinesterase intoxication (reviewed by Kaufer et al., 1999). It is noteworthy that transgenic mice overexpressing very high levels of AChE-R (Sternfeld et al., 1998) display dramatic fourfold elevated NMJ densities (T. Evron and M. Soreq, unpublished observation).

Until recently, the low-level basal expression of AChE-R precluded characterization of this protein from natural sources. Nonetheless, heterologous expression studies demonstrated AChE-R to be a soluble, secreted, nonsynaptic, catalytically active form of the enzyme (Seidman et al., 1995). In microinjected *Xenopus* embryos, expression of AChE-R was restricted to secretory epidermal cells. This is consistent with our observations of induced AChE-R mRNA in tongue epithelium. However, the absence of significant AChE activity in the

tongue epithelium suggests that excess AChE-R is excreted from, rather than retained within, this tissue as well. Normally, the accumulation of AChE in mature NMJs is accomplished by focal transcription at subjunctional nuclei combined with restrictions on diffusion of AChE mRNA or protein to nonjunctional sites (Jasmin et al., 1993). The diffuse localization of overexpressed AChE-R mRNA and of AChE enzyme in transgenic and DFP-treated muscle is consistent with a nonjunctional disposition for this enzyme. Moreover, it suggests that transcription of AChE mRNA is activated following DFP in otherwise "quiescent" nonjunctional nuclei. Nevertheless, the extent of overexpressed AChE in transgenic mice displayed a downward trend during postnatal development. Our current findings indicate adjustments of the AChE feedback loop and would explain our previous detection of only slightly elevated AChE activity in muscles of adult transgenic mice (Andres et al., 1997).

Increased numbers of small neurites were associated with increased numbers of small, immature endplates in diaphragms of DFP and transgenic mice. This suggests that NMJ stress stimulates compensatory mechanisms designed to increase the number of functional synapses. I.p. injections of antisense oligonucleotides to AChE mRNA ameliorated both induced AChE overexpression and motor endplate expansion. Because oligonucleotides are not known to cross the blood–brain-barrier unassisted (Seidman et al., 1999), the observation that systemic administration of AS3 effectively blocked DFP-promoted synaptogenesis indicates a prominent role for muscle-derived AChE-R in this phenomenon. Neurite-growth-promoting functions attributed to the synaptic AChE-S variant were shown to be independent of catalytic activity (Sternfeld et al., 1998). In the current study, repeated DFP treatments were associated with elevated levels of AChE-R mRNA and enhanced neurite branching even though *de novo* synthesized enzyme would be rapidly inactivated by residual inhibitor. This is compatible with the idea that catalytically inactive AChE-R exerts morphogenetic activities on mammalian motoneurons. Moreover, recent studies in our laboratory demonstrate long-term (at least 1 mo) overproduction of AChE-R in brain following exposure to DFP (Friedman et al., manuscript in preparation). This could help explain the devastating myopathic effects of even a single exposure to this agent (Taylor, 1996). As DFP promotes overexpression of AChE in central neurons, the signal driving changes in neurite structure could originate from either the muscle or the motoneurons themselves. Similarly, the effects of DFP on muscle may reflect its status as a target tissue of neurons overexpressing AChE-R. This latter possibility suggests further studies into the potential effects of overexpressed neuronal AChE on other target tissues such as adrenal gland and intestine.

A massive and transitory increase in *c-fos* mRNA and Fos protein was reported to occur in rats intoxicated by a single dose of Soman, a highly toxic irreversible inhibitor of cholinesterase (Chollat et al., 1993). In our study, both DFP and transgenic AChE promoted elevated levels of c-fos mRNA in muscle. Upregulation of this nuclear transcription factor could be owing to muscle necrosis and cell death because chronic elevation of Fos usually accompanies cell injury or apoptosis (Slotkin et al., 1997). However, induction of c-Fos was also reported to follow nerve growth factor administration in cholinergic neurons of the adult rat basal forebrain (Gibbs et al., 1997). Therefore, elevated c-fos mRNA in transgenic and DFP-treated mouse muscle could reflect regeneration processes. In brain, calcium-dependent elevations in *c-fos* mRNA were spatiotemporally correlated with elevated levels of AChE-R mRNA. This suggests that AChE-R represents a downstream, stress-responsive element in the nervous system. The sequence homology (de la Escalera et al., 1990; Ichtchenko et al., 1995) and functional redundancy (Darboux et al., 1996; Grifman et al., 1998) between AChE and neuronal cell-cell interaction proteins with protruding intracellular domains such as neurotactin and neuroligin suggest a role for AChE in cell adhesion. In that case, stress-responsive AChE-R could play a role in the neuronal remodeling that follows various stress insults. The core domain of AChE is likely to mediate the enzyme's noncatalytic functions, perhaps by regulating ligand-binding interactions between its homologous cell surface proteins and their natural binding partners (i.e., neurexins). Nevertheless, isoform-specific influences of AChE on cellular morphogenesis implies important, but yet undefined roles for the various alternative C-terminal peptides.

Cholinesterase inhibitors are routinely employed to treat various neurological disorders associated with cholinergic deficits. For example, the fluctuating muscle weakness suffered by individuals afflicted with myasthenia gravis is treated with chronic administration of neostigmine. Nevertheless, neostigmine has long been known to promote ultrastructural abnormalities of the postsynaptic NMJ membrane, terminal nerve branching, and myopathologies in normal rats (Engel et al., 1973; Hudson et al., 1978). For these reasons, it was suggested that anticholinesterase therapy may actually contribute to the progressive deterioration of muscle function in myasthenia gravis (Swash, 1975). Our current findings suggest that adverse responses to neostigmine might be mediated by feedback responses to AChE inhibition and consequent accumulation of AChE-R in muscle. Thus, our data point to feedback overexpression of AChE-R as a mechanism translating diverse physiological NMJ stresses into long-term neuromuscular pathologies. They therefore raise serious concern about excessive use of anticholinesterases for management of noncrisis medical situations. Perhaps it is not surprising, therefore, that muscle weakness is prominent among the complaints of Gulf War veterans having received 90 mg/d pyridostigmine as a prophylactic guard against anticipated exposure to chemical weapons (Haley et al., 1997). Thus, the indications that anticholinesterase drugs initiate potentially devastating feedback responses in mammalian muscle carries profound health implications for the relatively large group of individuals currently receiving, or targeted for, various anticholinesterase therapeutics. For example, the only drugs currently approved for Alzheimer's disease are potent AChE inhibitors. The efficient in vivo suppression of AChE overexpression achieved here with extremely low doses of antisense oligonucleotides to AChEmRNA suggests that antisense therapeutics may offer a viable alternative approach to conventional anticholinesterase therapy in the nervous system.

Acknowledgments

The authors would like to thank Drs. Asher Meshorer and Naomi Melamed-Book for helpful discussions and Ms. M. Maman-Sapir and Ms. D. Nathan, for excellent technical assistance. This research has been supported by the US Army Medical Research and Development Command (DAMD 17-99-1-9547), The Israel Science Foundation (590/97), and the US-Israel Binational Science Foundation (96-001100) (to H.S.).

References

Andres C., Beeri R., Friedman A., Lev-Lehman E., Henis S., Timberg R., et al. (1997). Acetylcholinesterase-transgenic mice display embryonic modulations in spinal cord choline acetyltransferase and neurexin Ibeta gene expression followed by late-onset neuromotor deterioration. *Proc. Natl. Acad. Sci. USA* **94,** 8173–8178.

Andres C., Seidman S., Beeri R., Timberg R., and Soreq H. (1998) Transgenic acetylcholinesterase induces enlargement of murine neuromuscular junctions but leaves spinal cord synapses intact. *Neurochem Int.* **32,** 449–456.

Ben Aziz Aloya R., Seidman S., Timberg R., Sternfeld M., Zakut H., and Soreq H. (1993). Expression of a human acetylcholinesterase promoter-reporter construct in developing neuromuscular junctions of Xenopus embryos. *Proc. Natl. Acad. Sci. USA* **90,** 2471–2475.

Chollat Namy A., Delamanche I. S., and Bouchaud C. (1993) Variation in the expression of c-fos after intoxication by soman. Comparative study using in situ hybridization and immunohistochemistry. *Brain Res.* **603,** 32–37.

Darboux I., Barthalay Y., Piovant M., and Hipeau Jacquotte R. (1996) The structure-function relationships in Drosophila neurotactin show that cholinesterasic domains may have adhesive properties. *EMBO J.* **15,** 4835–4843.

de la Escalera S., Bockamp E. O., Moya F., Piovant M., and Jimenez F. (1990) Characterization and gene cloning of neurotactin, a Drosophila transmembrane protein related to cholinesterases. *EMBO J.* **9,** 3593–3601.

Donger C., Krejci E., Serradell A. P., Eymard B., Bon S., Nicole S., et al. (1998). Mutation in the human acetylcholinesterase-associated collagen gene, COLQ, is responsible for congenital myasthenic syndrome with end-plate acetylcholinesterase deficiency (Type Ic). *Am. J. Hum. Genet.* **63,** 967–975.

Engel A. G., Lambert E. H., and Santa T. (1973) Study of long-term anticholinesterase therapy. Effects on neuromuscular transmission and on motor end-plate fine structure. *Neurology* **23,** 1273–1281.

Engelhardt J. I., Siklos L., and Appel S. H. (1997) Immunization of guinea pigs with human choline acetyltransferase induces selective lower motoneuron destruction. *J. Neuroimmunol.* **78,** 57–68.

Evoli A., Batocchi A. P., and Tonali P. (1996) A practical guide to the recognition and management of myasthenia gravis. *Drugs* **52,** 662–670.

Friedman A., Kaufer D., Shemer J., Hendler I., Soreq H., and Tur Kaspa I. (1996). Pyridostigmine brain penetration under stress enhances neuronal excitability and induces early immediate transcriptional response. *Nat. Med.* **2,** 1382–1385.

Gibbs R. B. and Martynowski C. (1997). Nerve growth factor induces Fos-like immunoreactivity within identified cholinergic neurons in the adult rat basal forebrain. *Brain Res.* **753,** 141–151.

Grifman M., Galyam N., Seidman S., and Soreq H. (1998) Functional redundancy of acetylcholinesterase and neuroligin in mammalian neuritogenesis. *Proc. Natl. Acad. Sci. USA* **95,** 13,935–13,940.

Grisaru D., Lev-Lehman E., Shapira M., Chaikin E., Lessing J. B., Eldor A., et al. (1999) Human osteogenesis involves differentiation-dependent increases in the morphogenically active 3′-alternative splicing variant of acetylcholinesterase. *Mol. Cell Biol.* **19,** 788–795.

Haley R. W., Kurt T. L., and Hom J. (1997) Is there a Gulf War Syndrome? Searching for syndromes by factor analysis of symptoms. *JAMA* **277,** 215–222.

Hudson C. S., Rash J. E., Tiedt T. N., and Albuquerque E. X. (1978) Neostigmine-induced alterations at the mammalian neuromuscular junction. II. Ultrastructure. *J. Pharmacol. Exp. Ther.* **205,** 340–356.

Ichtchenko K., Hata Y., Nguyen T., Ullrich B., Missler M., Moomaw C., and Sudhof T. C. (1995). Neuroligin 1: a splice site-specific ligand for beta-neurexins. *Cell* **81,** 435–443.

Jasmin B. J., Lee R. K., and Rotundo R. L. (1993) Compartmentalization of acetylcholinesterase mRNA and enzyme at the vertebrate neuromuscular junction. *Neuron* **11,** 467–477.

Kaufer D., Friedman A., and Soreq H. (1999) The vicious circle of stress and anticholinesterase responses. *Neuroscientist* **5,** 173–183.

Kaufer D., Friedman A., Seidman S., and Soreq H. (1998) Acute stress facilitates long-lasting changes in cholinergic gene expression. *Nature* **393,** 373–377.

Kawabuchi M., Osame M., Watanabe S., Igata A., and Kanaseki T. (1976) Myopathic changes at the endplate region induced by neostigmine methylsulfate. *Experientia* **32,** 632–635.

Koenigsberger C., Chiappa S., and Brimijoin S. (1997) Neurite differentiation is modulated in neuroblastoma cells engineered for altered acetylcholinesterase expression. *J. Neurochem.* **69,** 1389–1397.

Laskowski M. B., Olson W. H., and Dettbarn W. D. (1975) Ultrastructural changes at the motor endplant produced by an irreversible cholinesterase inhibitor. *Exp. Neurol.* **47,** 290–306.

Layer P. G. and Willbold E. (1995) Novel functions of cholinesterases in development, physiology and disease. *Prog. Histochem. Cytochem.* **29,** 1–99.

Lindstrom J. (1998) Mutations causing muscle weakness. *Proc. Natl. Acad. Sci. USA* **95,** 9070,9071.

Livneh A., Sarova I., Michaeli D., Pras M., Wagner K., Zakut H., and Soreq H. (1988). Antibodies against acetylcholinesterase and low levels of cholinesterases in a patient with an atypical neuromuscular disorder. *Clin. Immunol. Immunopathol.* **48,** 119–131.

Massoulie J., Pezzementi L., Bon S., Krejci E., and Vallette F. M. (1993) Molecular and cellular biology of cholinesterases. *Prog. Neurobiol.* **41,** 31–91.

Sanes J. R. and Lichtman J. W. (1999) Development of the vertebrate neuromuscular junction. *Ann. Rev. Neurosci.* **22,** 389–442.

Schonbeck S., Chrestel S., and Hohlfeld R. (1990) Myasthenia gravis: prototype of the antireceptor autoimmune diseases. *Int. Rev. Neurobiol.* **32,** 175–200.

Seidman S., Sternfeld M., Ben Aziz Aloya R., Timberg R., Kaufer Nachum D., and Soreq H. (1995). Synaptic and epidermal accumulations of human acetylcholinesterase are encoded by alternative 3′-terminal exons. *Mol. Cell Biol.* **15,** 2993–3002.

Seidman S., Eckstein F., Grifman M., and Soreq H. Antisense technologies have a future combating neurodegenerative disease. *Antisense Res. Drug Dev.* **9,** 333–340.

Shapira M., Seidman S., Sternfeld M., Timberg R., Kaufer D., Patrick J., and Soreq H. (1994). Transgenic engineering of neuromuscular junctions in *Xenopus laevis* embryos transiently overexpressing key cholinergic proteins. *Proc. Natl. Acad. Sci. USA* **91,** 9072–9076.

Sharma K. V. and Bigbee J. W. (1998) Acetylcholinesterase antibody treatment results in neurite detachment and reduced outgrowth from cultured neurons: further evidence for a cell adhesive role for neuronal acetylcholinesterase . *J. Neurosci. Res.* **53,** 454–464.

Slotkin T. A., McCook E. C., and Seidler F. J. (1997) Cryptic brain cell injury caused by fetal nicotine exposure is associated with persistent elevations of c-fos protooncogene expression. *Brain Res.* **750,** 180–188.

Sternfeld M., Ming G., Song H., Sela K., Timberg R., Poo M., and Soreq H. (1998). Acetylcholinesterase enhances neurite growth and synapse development through alternative contributions of its hydrolytic capacity, core protein, and variable C termini. *J. Neurosci.* **18,** 1240–1249.

Sternfeld M., Patrick J. D., and Soreq H. (1998) Position effect variegations and brain-specific silencing in transgenic mice overexpressing human acetylcholinesterase variants. *J. Physiol.* (Paris) **92,** 249–255.

Swash M. (1975) Motor innervation of myasthenic muscles (Letter). *Lancet* **2,** 663.

Taylor P. (1996) Agents acting at the neuromuscular junction and autonomic ganglia, in *Goodman and Gilman's The Pharmacological Basis of Therapeutics* (Hardman J. G., Limbird L. E., Molinoff P. B., and Ruddon R. W., eds.), McGraw-Hill, New York, pp. 177–197.

Taylor P., Radic Z., Hosea N. A., Camp S., Marchot P., and Berman H. A. (1995). Structural bases for the specificity of cholinesterase catalysis and inhibition. *Toxicol. Lett.* 82–83, 453–458.